

Research on the closed loop micro-/nano-positioning stage for z-axis scanning using the real time control system

Fang-Jung Shiou¹, Chao-Jung Chen², Jyun-Da Huang¹, Huay-Chung Liou²

¹ Department of Mechanical Engineering, National Taiwan University of Science and Technology, 43, Keelung road, section 4, Taipei, 106, Taiwan

² Center for Measurement Standards, Industrial Technology Research Institute (ITRI), 3 321, Kuang-Fu Road, Section 2, Hsinchu, 300 Taiwan

Corresponding Author: E-mail: shiou@mail.ntust.edu.tw, TEL: +886-2-2737-6543, FAX: +886-2-2737-6460

KEYWORDS: Micro-/nano-positioning stage, ANSYS software, lever displacement magnification mechanism, capacitive sensor system, PID control

The aim of this research is to develop a NI cRIO real time based closed loop micro-/nano-positioning system for z-axis scanning. The developed system mainly consists of a piezoelectric actuator, a lever mechanism for displacement magnification, a coaxial symmetric flexible stage analyzed by the FEM software ANSYS, capacitive sensors, NI cRIO Real-Time control interface, and a PC. A set of software written with the LabView programming language was developed to construct the PID closed-loop control of the developed positioning system. A lever displacement magnification mechanism has been designed to enlarge the travel of PZT actuator. After executing the simulation analyses of the displacement, stress, and the natural frequency, using the ANSYS software, the dimensions of the lever displacement magnification mechanism have been designed and determined. Test results show the positioning stage can achieve a travel range of 104.4 μm in vertical direction. The positioning resolution was about 2.5 nm and tracing speed was 10 $\mu\text{m/s}$ by the NI cRIO real-time based PID control. The maximum angular deviation in Y-direction was about 5.81 μrad .

Manuscript received: January XX, 2011 / Accepted: January XX, 2011

NOMENCLATURE

K_d = stiffness of the leaf spring

K_p , K_i and K_D = the controller gains of the error signal

L = length of the lever spring

L_1 = distance between the lever spring and the PZT actuator

1. Introduction

Micro/nano-positioning stage plays an important role in the semiconductor technology, biotechnology, micro-/nanofabrication, microscopy, metrology, precision machining, etc. The piezoelectric transducer (PZT) has been extensively applied as the actuator of a micro-/nano-positioning stage. Types of micro-/nano-positioning stages using PZT can basically be divided into three categories: 1. direct-drive piezo actuators, 2. piezo-driven flexure, and 3. ultrasonic piezomotors [1]. Vertical piezo-driven flexure nano-positioning scanning stages can be applied to the high precision measurement systems, such as: white light interferometry, autofocus systems, confocal microscopy, etc. The travel of the most of the direct-drive piezo actuators are, in general, within tens of microns with resolution of sub-nanometer [2]. Through the flexure design of a lever magnification, the travel over 100 microns driven by a PZT was possible [1]. The travel of a stage was magnified via the design of a series of two lever flexures [3]. The Scott-Russell mechanism and the leaf spring flexure was applied in [4], to increase the travel of a piezo-

driven stage and to eliminate the angular errors and lateral movement error of the stage during positioning. A novel open-loop long-travel piezoelectric-driven linear nano-positioning stage using the toggle amplification mechanism has been presented to eliminate the lateral offset error of the level mechanism in [5]. The flexure hinges were used in most of the mentioned piezo-driven stages. Capacitive and inductive sensors are commonly used as feedback sensors for closed-loop control of some micro-/nano-positioning stages [6]. How to design a closed loop vertical fast micro-/nano-positioning stage with real time control was not investigated based on the literature review.

The aim of this research is to design a real time based closed-loop micro-/nano-positioning stage for z-axis scanning and to integrate a capacitive with the stage body as the feedback sensor. The detailed design and manufacture of a closed-loop micro-/nano-positioning stage embedded with a capacitive sensor was introduced in section 2. The control loop of the developed system was presented in section 3. The experimental results including the step-positioning, the slope-tracing, and the tilting angles measurement, respectively, were illustrated in section 4.

2.Designand Manufacture of a Closed-Loop Micro-/Nano-Positioning Stage

2.1 Design of the Micro-/Nano-Positioning Stage System

Figure 1 shows the exploded illustration of the designed micro-/nano-positioning stage. The developed positioning system mainly consists of a piezoelectric actuator, a lever (Y-part) for displacement magnification mechanism, a micro-/nano-positioning stage body constrained by two flat springs, each flat spring with four symmetric leaf springs, a capacitive sensor, and a PC. The open loop travel of the used PZT, a product of Piezsystem Jena[7], was $28\ \mu\text{m} + 10\%$ with an input voltage of 100 V, and the stiffness was $100\ \text{N}/\mu\text{m}$. The movement of the designed micro-/nano-positioning stage body was constrained by two sets of flat springs each with four leaf springs. The displacement magnification ratio of the lever was about a factor of four. A capacitive sensor, a product of PI Instrument, was integrated with the stage as a position feedback sensor, so that the closed-loop control was possible.

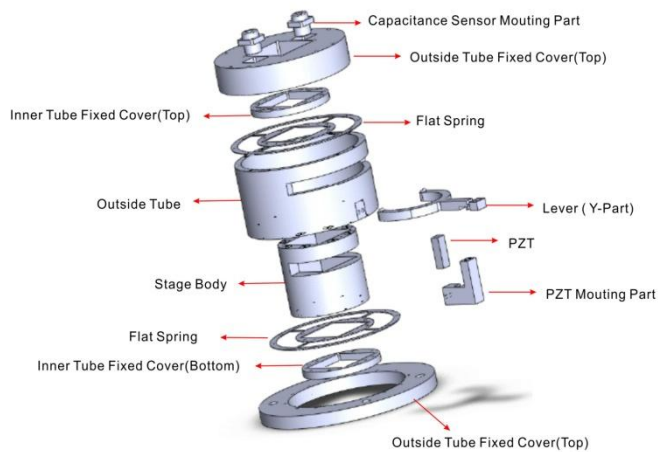


Fig.1 Exploded view of the micro-/nano-positioning stage system

2.2Design Of The Micro-/Nano-Positioning Stage System

To optimize the geometric dimensions of the leaf springs of the stage body, the ANSYS software was applied to analyze the stress, displacement, and the frequency of the stage actuated by the PZT. In general, the process of optimization analysis using the ANSYS software can be summarized as follows [8]:

- (1). Modeling of the designed object, setting parameters (such as element type, real constants, and material properties), meshing of the designed object, setting of the constraints (boundary conditions) and the loads using the pre-processor.
- (2). Find the static solution after determining the analysis type using the solution processor.
- (3). Display the analysis results using the general post-processor.
- (4). Set the objective function, design variables, and constraints for optimization analysis.
- (5). Execution of the optimization analysis using the design optimization processor.
- (6). Evaluation of the optimization analysis results.

Figure 2 shows the model of the stage body with two sets of flat springs constructed with the ANSYS software. The ANSYS 3-D Structural Solid Element Brick 8 Node 45 (SOLID 45) was selected as the meshing element type to construct the model. The selected material of the stage was aluminium alloy T6-6061. The Young's modulus of $71 \times 10^9\ \text{N}/\text{m}^2$, the density of $2700 \times 10^{-9}\ \text{kg}/\text{m}^3$, and the Poisson's ratio of 0.33, have been set as the material properties. After the model had been constructed and the parameters had been set, the meshing of the stage has been carried out. The translation and rotation of the outside tube, used for mounting, have been set fixed as boundary conditions. By setting the analysis type of the solution processor as static, the solution of the desired node could then be determined.

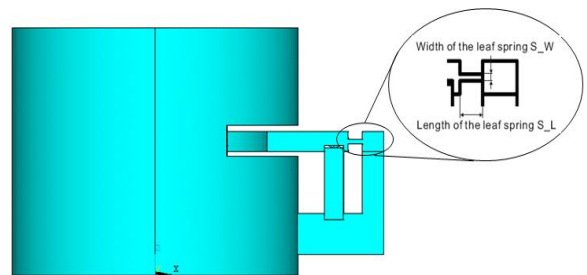


Fig.2Modeling of the stage body with two sets of flat springs using ANSYS software

Having set the movement of 100 microns of the stage along vertical direction as the objective function, four variables, namely the width, length, thickness of the lever (Y-part), the activating position of the PZT on the lever as the design variables, and the induced maximum stress, which was smaller than the yielding stress of $143.3 \times 10^6\ \text{N}/\text{m}^2$ of the used material T6-6061 with a safety factor of 1.5, as the constraints, the optimization process has been carried out. The geometric dimensions of the level spring after executing the iterative optimization process after configuring the appropriate range of the dimensions. The maximum induced stress of the stage was $83.4 \times 10^6\ \text{N}/\text{m}^2$ (Fig. 3) as the travel of the stage was 102 microns (Fig. 4)

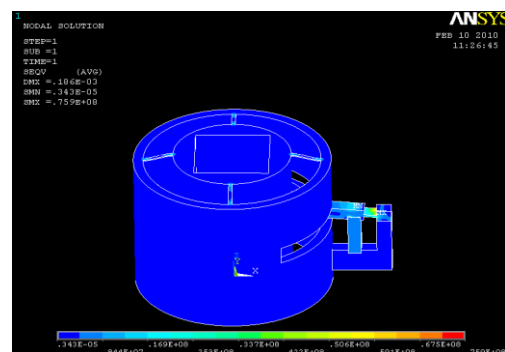


Fig. 3 Simulation results of the designed stage: Stress distribution

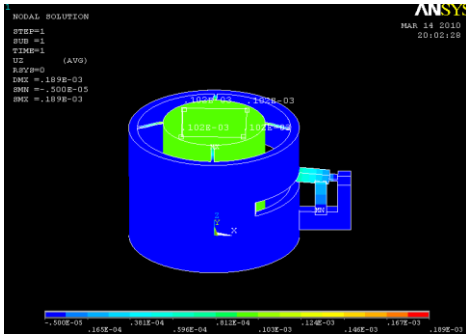


Fig. 4 Simulation results of the designed stage: displacement distribution

2.3 Natural frequency analysis of the stage

In order to find the natural frequency of the developed stage, the simulation, calculation and hammer test, respectively, have been carried out in this study. The intention was that the resonance of the stage body could be avoided. Using the model analysis of the ANSYS software, the natural frequency of the developed stage could be extracted, as shown in Fig. 5. The frequency was around 41.2 Hz for the 1st mode. The measured natural frequency was about 45 Hz using the hammer test. With the load of 2 kg for the lens and camera, the simulated frequency was around 30 Hz.

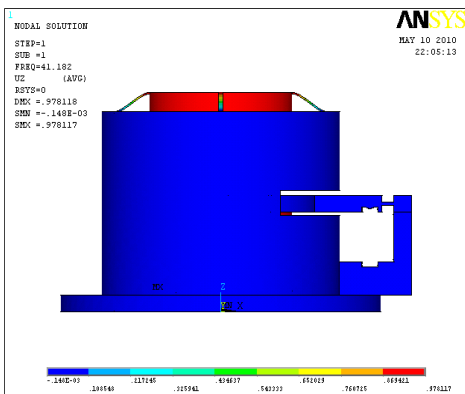


Fig. 5 Simulation results of the natural frequency (41.2 Hz)

In order to find the displacement of the developed stage using the calculation method, the simplified model of stage with two sets of flat springs is shown in Fig. 6 by neglecting the friction force and the excitation force activated by the lever for displacement magnification mechanism. The derived displacement of the stage body is listed in equation (2-1).

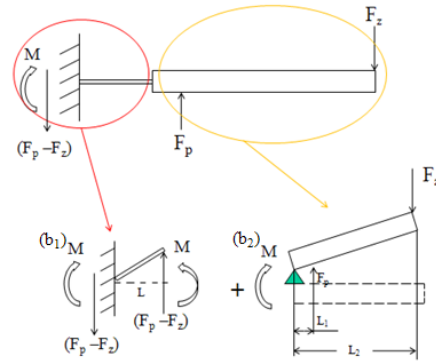
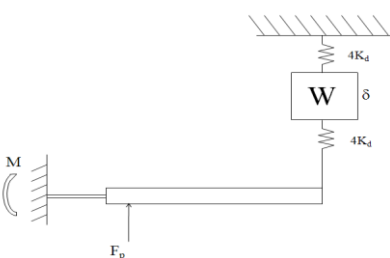


Fig. 6 Simplified model of the stage to derive the displacement of the stage body

$$\delta = (2-1) \frac{1}{8K_d} \times \left(\frac{F_p(L_1 + L)}{(L + L_2)} - \frac{M}{(L + L_2)} \right)$$

2.4 Developed micro-/nano-positioning stage

The geometrical dimensions of the leaf spring having been determined by executing the iterative optimization analyses, the stage body was fabricated by the wire electrical discharge machining (EDM) process. Based on the design configuration of the positioning system (Fig. 1), the piezoelectric actuator, the lever (Y-part), two flat springs, and the capacitive sensor were integrated with the fabricated stage body. The assembled micro-/nano - positioning stage mounted on an optical table is shown in Fig. 7.

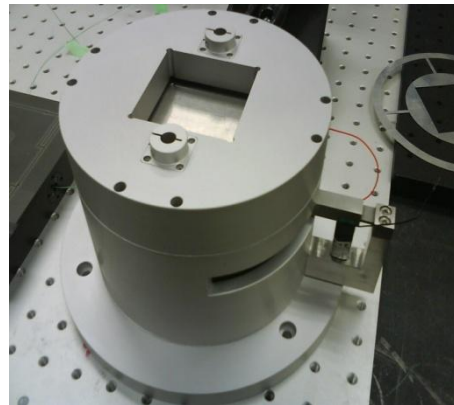


Fig.7 Photo of the developed micro-/nano-positioning stage system mounted on an optical table

3. Closed-Loop Control of the Developed System

To overcome the hysteresis and nonlinearity of the PZT, about 10% of the travel, a closed-loop control has been applied to the micro-/nano-positioning stage system. Fig. 8 shows the feedback loop of the stage system. The positioning stage was driven by the PZT actuator, model of P-233-40.N40/S10, made by Piezsystem Jena. The PZT actuator was driven by the PZT driver from 0 V to 100 V. The PZT driver was controlled by the PID controller of the PC through a D/A interface card, model of NI 9263, made by NI Co. The precise movement of the positioning stage was monitored by the capacitive sensor. The outputs of the capacitive sensor were connected to the

capacitive sensor amplifier E-853 connected to an analog to digital conversion (A/D) interface card, model of NI 9215 made by NI Co.. A set of software, written with the LabView programming language, was developed to conduct the PID control of the positioning stage. A real time controller, model of NI cRIO 9074 with Xilinx FPGA processor [9], was used to deal with the input and output signal processing to speed up the positioning of the stage body, as shown in Fig. 9.

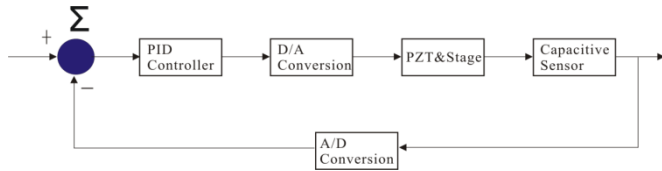


Fig.8 Feedback loop of the micro-/nano-positioning stage system

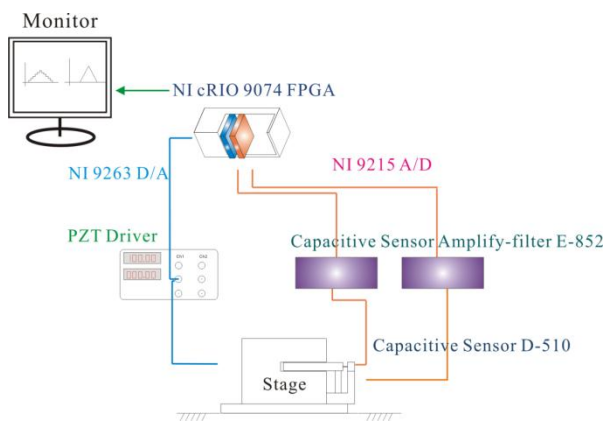


Fig.9 Schematic illustration of the micro-/nano-positioning stage system

The proportional integral derivative (PID) control algorithm has been used to the closed-loop control. The error signal $e(t)$ was the difference between the target position and the measured position. The voltage $u(t)$ input to the PZT driver can be expressed as follows:

$$u(t) = K_p e(t) + K_i \int_0^t e(t) dt + K_D (\dot{e}(t) - \dot{e}(t-1)) \quad (3-1)$$

Where, K_p , K_i and K_D are the controller gains of the error signal, the integral of the error signal, and the first derivative of the error signal, respectively.

4. Experimental Results

To evaluate the performance of the developed closed-loop positioning stage, experiments were carried out on the tracing speeds, the tilting angles using different hinges, step-positioning, and slope-tracing, respectively. The controller gains of the PID control were set as $K_p=0.15$, $K_i=5.5$, and $K_D=0.001$, based on the iterative test results [10], so that there was almost no overshoot and response delay, as shown in Fig. 10. Different speeds for slope tracing, such as 1000 nm/s, 5,000 nm/s, 8,000 nm/s, and 10,000 nm/s, have been executed in order to determine an appropriate tracing speed. The greater the tracing speed, the greater the positioning delay, based on the results of the experiments [10]. There was almost no positioning delay using the tracing speed of 10,000 nm/s. As a result, this tracing

speed was applied to the tilting angles test, step-positioning test, and slope-tracing test. Fig. 11 shows the results of the step-positioning of 10 μm of the developed stage. An error of about ± 2 nm measured with the capacitive sensor is shown in Fig. 12.

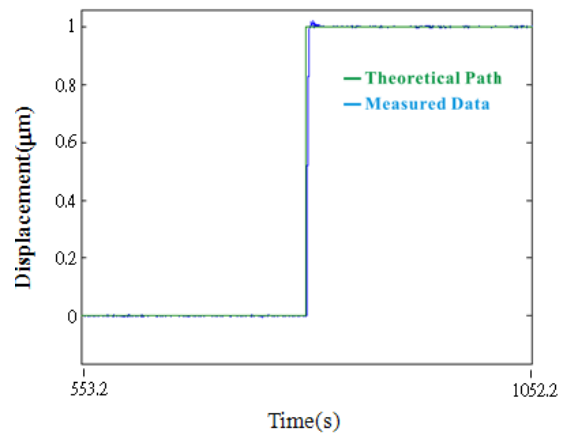


Fig.10 Step tracing result of the step-positioning of 1 μm

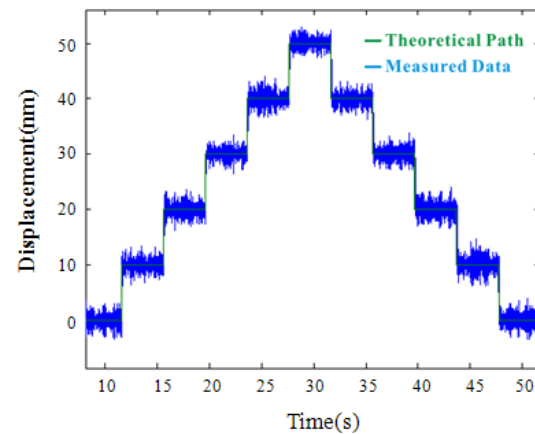


Fig.11 Results of the step-positioning of 10 μm

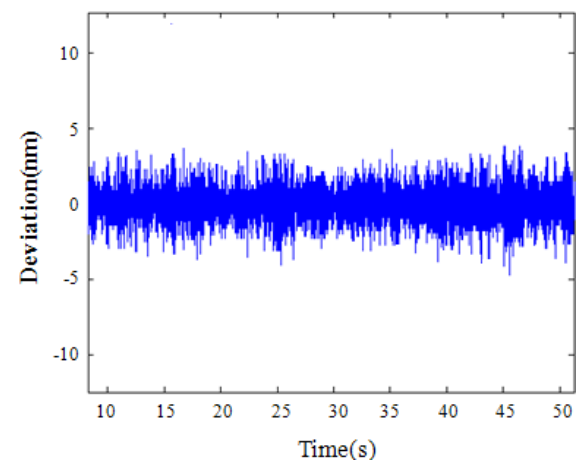
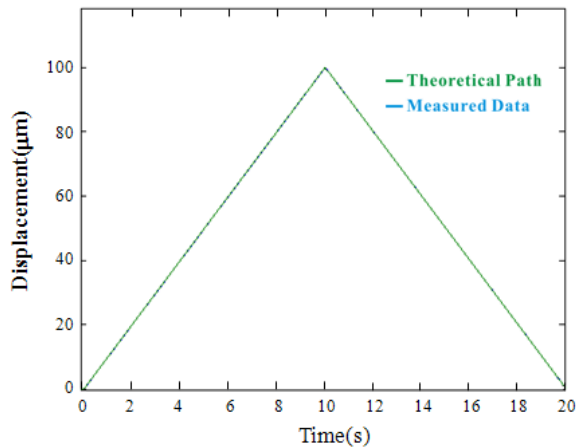
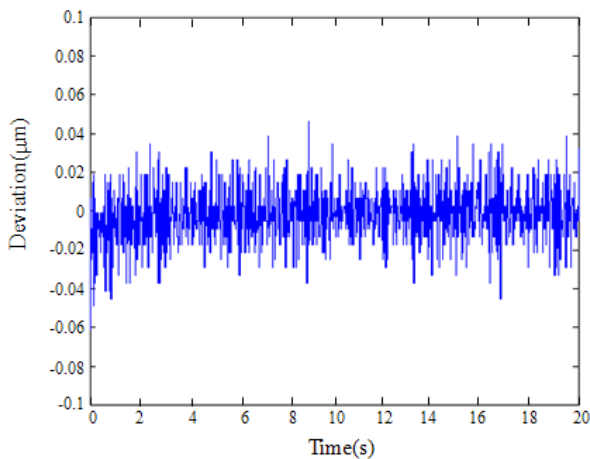


Fig.12 Error plot of the step-positioning of 10 μm

Figure 13 shows the results of slope-tracing of 100 μm of the developed stage. An error about ± 20 nm measured with the capacitive sensor system is shown in Fig. 14.

Fig.13 Result of slope-tracing of 100 μm Fig.14 Error plot of slope-tracing of 100 μm

The tilting angles of the developed stage were measured with an autocollimator with a resolution of 0.001 arc-second. Figure 15 shows different tilting angles of the stage with respect to the x-, y-, and z-axis, respectively. The smaller the displacement, the smaller the tilting angles. The maximum angular deviation in Y-direction was about 5.82 μrad .

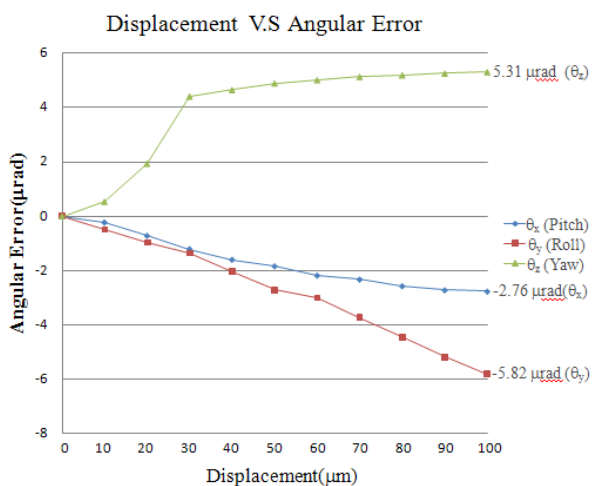


Fig. 15 Measured tilting angles of the developed stage

5. Conclusion

A prototype of the NI cRIO real time based closed-loop micro-/nano-positioning stage for z-axis scanning, integrated with a capacitive sensor, has been newly developed. The geometric dimensions of the lever spring were determined by executing the optimization analysis using the ANSYS software. A closed-loop PID controller has been applied to the micro-/nano-positioning stage system, to overcome the hysteresis and nonlinearity of the PZT. According to the test results, the positioning stage can achieve a travel range of 104.4 μm in vertical direction. The positioning resolution was about 2.5 nm and tracing speed was 10 $\mu\text{m/s}$ using the NI cRIO real-time based PID control. The maximum angular deviation in Y-direction was about 5.81 μrad . However, the volume of the developed stage and the positioning accuracy could be further improved in the future work.

ACKNOWLEDGEMENT

The authors are appreciative to the National Science Council of the Republic of China for partially supporting this research under grant NSC 98-2221-E-011-100-MY2.

REFERENCES

1. PI, 20118, Available: <http://www.physikinstrumente.com/>
2. Yin, C., Lin, D., Wu, J., and Zhang, R., "Design and detection of super-precision positioning stage with nanometer resolution," Proceedings of SPIE - The International Society for Optical Engineering, Vol. 4444, pp. 350-357, 2001.
3. Ryu, J. W., Gweon, D. G., and Moon, K. S., "Optimal design of a flexure hinge based XY θ wafer stage," Precision Engineering, Vol. 19, pp. 18-28, 1997.
4. Chang, S. H., and Du, B. C., "A precision piezodriven micropositioner mechanism with large travel range," Review of Scientific Instruments, Vol. 69, pp. 1785-1791, 1998.
5. Chu, C. L., and Fan, S. H., "A novel long-travel piezoelectric-driven linear nanopositioning stage," Precision Engineering, Vol. 30, pp. 85-95, 2006.
6. Sebastian, A., and Salapaka, S. M., "Design methodologies for robust nano-positioning," IEEE Transactions on Control Systems Technology, Vol. 13, No.6, 868-876, 2005.
7. Piezosystem Jena, "Hysteresis Protocol", Piezosystem Jena company, 2009
8. ANSYS, User's Manual of ANSYS 8.0, ANSYS, Corp., Canonsburg, PA, USA, 2006.
9. National Instruments, "CompactRIO and LABVIEW Development Fundamentals", 2007
10. Huang, J. D., "Research of the closed-loop micro-/nano- Z-Axis positioning stage using the real-time control system," Master thesis (in Chinese), National Taiwan University of Science and Technology, Taiwan, 2010.